Geochimica et Cosmochimica Acta, Vol. 69, No. 12, pp. 2959–2969, 2005

0016-7037/05 $30.00 + .00

doi:10.1016/j.gca.2005.01.017

The effects of solution chemistry on the sticking efficiencies of viable *Enterococcus faecalis*: An atomic force microscopy and modeling study

Tracy L. Cail,*,† and Michael F. Hochella, Jr.
Department of Geosciences, 4044 Derring Hall, Virginia Tech, Blacksburg, Virginia 24061-0420, USA

(*Received October* 25, 2004; *accepted in revised form January* 18, 2005)

Abstract—Atomic force microscopy (AFM) and Derjaguin-Landau-Verwey-Overbeek (DLVO) theory in combination with the interaction force boundary layer (IFBL) model have been used to empirically and theoretically calculate sticking efficiencies (α) of *Enterococcus faecalis* cells against a silica glass surface. Sticking efficiencies were calculated in solutions of varying pH and ionic strength and related to maximum distances of transport through a hypothetical soil block using colloid filtration theory.

AFM measurements show that the repulsive and attractive forces between *E. faecalis* cells and a glass surface are a function of ionic strength but are less sensitive to changes in solution pH. Zeta (ζ)-potential measurements of the cells and glass surfaces correlate with these trends. Calculated DLVO energy profiles predict much greater sensitivity to changing solution chemistry. Sticking efficiencies derived from AFM measurements range from 9.6×10^{-17} to 1 in solutions of low ionic strength (IS) and from 2.6×10^{-33} to 1 at higher IS. Corresponding α values determined from DLVO theory are essentially zero in all tested solutions.

Sticking efficiencies calculated in this study are smaller than values determined from column and field studies in similar systems; however, α derived from AFM data and the IFBL model more closely represent field data than do values calculated from DLVO energy values. A comparison with different methods of calculating α suggests that reversible adhesion may be significant in column-scale transport studies.

1. INTRODUCTION

Microbes are ubiquitous: They exist, and often thrive, in nearly every imaginable environment on Earth. It is estimated that 5×10^{30} prokaryotes exist on Earth and although less than 1% of that total number, including both *Bacteria* and *Archaea*, are freely suspended in groundwater, almost 50% are attached to unconsolidated sediment in the terrestrial subsurface (Whitman et al., 1998). The adhesion of microorganisms to unconsolidated sediment surfaces has widespread consequences and/or applications in the natural environment including mineral dissolution, contaminant stabilization and destabilization, microbe-facilitated or microbe-impeded contaminant transport, and public health. The processes that control the attachment of microbes to mineral surfaces are therefore important factors that control contaminant migration and resilience in the subsurface. It is vital that we understand how microbes and other colloid-sized particles attach to and detach from natural sediments and ultimately how they are transported through porous media.

Colloidal particles, such as prokaryotes, are transported through porous media by convective diffusion and are removed from suspension predominately by filtration (Yao et al., 1971). Several models that describe particle transport through unconsolidated media have been developed (for a review see Logan, 1999); however most are constrained to very specific physical and chemical conditions and few apply to real heterogeneous systems. Very few descriptions of particle transport account for the nanoscale interactions, including both attractive and repulsive interactions, which control particle attachment to surfaces.

One factor that is used to estimate colloidal particle attachment is sticking efficiency (α), which is defined as the fraction of particles colliding with a collector surface that remain attached to that surface. Accurate predictions of sticking efficiency are vital to successfully modeling particle transport in natural sediments. Unfortunately, there is rarely any agreement between predicted and measured transport of colloidal particles in real systems (Tobiason, 1989), and there are no published reports that successfully predict bacterial transport in aquifer materials based on independently determined sticking efficiencies (Harvey and Harms, 2002).

The goal of this research is to investigate particle adhesion at the nanoscale and to relate it to the large scale phenomenon of particle transport. In this study, sticking efficiency was calculated using forces measured by atomic force microscopy (AFM) and applied to the interaction force boundary layer (IFBL) model of Spielman and Friedlander (1974). Specifically, the sticking efficiencies of live *Enterococcus faecalis* cells adhering to a glass collector were examined in aqueous solutions of varying pH and ionic strength. Zeta (ζ)-potential measurements were used to qualitatively predict the electrostatic interactions between *E. faecalis* cells and a glass collector and to help rationalize the relationship between bacterial adhesion and solution chemistry. Sticking efficiencies calculated using AFM data and the IFBL model were then compared to values calculated using Derjaguin-Landau-Verwey-Overbeek (DLVO) theory and the IFBL model. Finally, sticking efficiencies were related to particle travel distances through a hypothetical soil block and compared to field studies.

* Author to whom correspondence should be addressed (banktl@ornl.gov).
† *Present address:* Environmental Sciences Division, Oak Ridge National Lab, Oak Ridge, Tennessee, 37831-6038, USA.

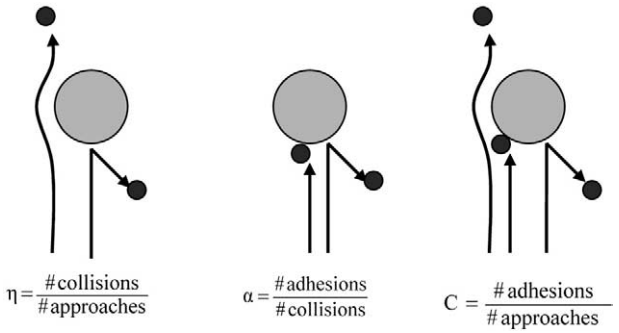

Fig. 1. Schematic representations of collision (η), sticking (α), and collection (C) efficiencies that are used in this paper.

This research is the first to use the IFBL model and AFM measurements to calculate sticking efficiencies of live bacterial cells and the first to provide a direct comparison of AFM- and DLVO-derived energy profiles of individual cells. The data are also presented as distances of travel through soil for a more lucid comparison with field data. The results of this study show that sticking efficiency estimates are sensitive to the methods used in their derivation.

2. BACKGROUND

2.1. Terminology

The terminologies that are used to describe the removal of colloidal particles from suspension by adhesion onto a collector surface are inconsistent in published literature and, at times, counterintuitive. The terms used in this paper are defined below. For clarity, Figure 1 illustrates the processes that are involved in particle transport and three key definitions.

2.1.1. *Collision efficiency (η)*

Collision efficiency (η), which is sometimes called collector or contact efficiency, is the probability that a particle approaching a collector surface collides with that surface. Because η is a probability, its value always falls between 0 and 1. Collision efficiency can be calculated using the Smoluchowski-Levich equation (Levich, 1962; Spielman and Friedlander, 1974):

$$\eta = 4A_s^{1/3}\left(\frac{D}{2Ur}\right)^{2/3} \quad (1)$$

where D is the particle diffusion coefficient, U is the undisturbed fluid velocity, and r is the particle radius (for units, see the list of symbols at the end of the article). A_s is Happel's cell model constant which is a porosity dependent flow model parameter that has a value of 38 for a given porosity of 0.4 (Elimelech and O'Melia, 1990a). Other forms of the Smoluchowski-Levich equation have been derived to include effects of particle-particle interactions (Logan, 1999).

2.1.2. *Sticking efficiency (α)*

Sticking efficiency, sometimes called sticking probability, attachment efficiency, or the collision efficiency factor, is a function of solution chemistry and the surface properties of the particle and collector. Estimates of α, which should always be between 0 and 1, have been obtained using colloid filtration theory (Yao et al., 1971), the kinetic energy (KE) method (Hahn and O'Melia, 2004), and the IFBL model (Elimelech and O'Melia, 1990a, 1990b; Dong et al., 2002b). There is wide variability in the published sticking efficiencies of similar systems that are calculated using these three methods (e.g., $\alpha_{IFBL} = 1 \times 10^{-181}$ and $\alpha_{KE} = 0.02$ Dong et al., 2002b).

2.1.3. *Collector efficiency (C)*

Collector efficiency is the combined probability that a particle approaching a collector surface both collides with and remains attached to the surface ($C = \eta\alpha$). It is the collector efficiency that ultimately describes the total removal of particles from solution and is used to predict total distances of particle transport (Yao et al., 1971). Collector efficiency is sometimes referred to as removal or deposition efficiency.

2.2. Interaction Force Boundary Layer Model

The IFBL model was derived by Spielman and Friedlander (1974) to describe spherical particle interactions with a spherical collector surface. Their model is specific to particles that are small enough to experience significant brownian motion, which limits the model to particles ≤ 2 μm in diameter (particles larger than 2 μm typically fall out of suspension owing to gravitational settling). The model assumes that particle-collector adhesion is irreversible and occurs when the potential energy between the particle and collector is minimized. The sticking efficiency is equal to the probability that a particle overcomes a potential energy barrier to reach a potential energy minimum. By definition of the IFBL model, particles and surfaces tht do not experience any interfacial repulsion have a sticking efficiency value of 1.

In the IFBL derivation, the convective diffusion equation with a term to describe particle-particle interactions is solved using two boundary conditions: (1) Convective transport is negligible when separation distances are extremely small, and (2) convective transport dominates over particle-particle interactions at large distances of separation. Details of the solution are available in Spielman and Friedlander (1974).

The IFBL model calculates sticking efficiencies as a function of the intersurface potential energy (ϕ) between a particle and collector. In this study, forces measured by AFM have been integrated over separation distance to obtain ϕ. Classical DLVO theory has also been used to calculate ϕ directly. The intersurface potential energy is integrated to calculate the surface reaction rate (k') which is the ratio of the rate of diffusive transfer of colloidal particles to the collector surface to the overall rate of adhesion:

$$k' = \frac{D}{\int_0^\infty (e^{\phi/kT} - 1)\,\partial\, y} \quad (2)$$

where D is the diffusion coefficient ($kT/6\pi\mu r$), k is Boltzmann's constant, T is temperature, μ is fluid viscosity, r is particle radius, y is the particle-collector separation distance, and ϕ is the intersurface potential energy. A modification to the rate of reaction equation that approximates the retarding effects

of hydrodynamics on particle mobility has been suggested (Dahneke, 1974):

$$k' = \frac{D}{\int_0^\infty \left[\left(1+\frac{r}{y}\right) * e^{\phi/kT} - 1\right] \partial y} \quad (3)$$

The surface reaction rate is then used in the IFBL model to determine the sticking parameter, β, which is defined by

$$\beta = \frac{1}{3}(2)^{1/3}\Gamma\left(\frac{1}{3}\right)A_s^{-1/3}\left(\frac{D}{Ur}\right)^{1/3}\left(\frac{k'r}{D}\right) \quad (4)$$

where Γ is the mathematical gamma function, A_s, D, U, and r are the Happel's cell model constant, diffusion coefficient, undisturbed velocity, and particle radius defined previously.

Finally, sticking efficiency is calculated from β using the equation

$$\alpha = \left(\frac{\beta}{\beta+1}\right) * S(\beta) \quad (5)$$

where $S(\beta)$ is a dimensionless function describing collection by a sphere. $S(\beta)$ has been determined numerically and is tabulated in Spielman and Friedlander (1974).

The IFBL model has been used to predict sticking efficiencies of live bacterial cells against quartz beads ($\alpha = 1 \times 10^{-181}$, Dong et al., 2002b), latex particles against glass ($\alpha = 1 \times 10^{-4}$, Elimelech and O'Melia, 1990a; $\alpha = 1 \times 10^{-4}$, Elimelech and O'Melia, 1990b), silica particles against glass ($\alpha = 1 \times 10^{-265}$, Elimelech et al., 2000), and silica particles against iron oxide coated sand ($\alpha = 0.3$, Ryan et al., 1999) in aqueous solutions of various pH and ionic strength. In many of these studies, theoretically calculated sticking efficiencies are several orders of magnitude lower than sticking efficiency values obtained from column and field-scale experiments in similar systems. Cited explanations for these discrepancies include failure of the DLVO theory to accurately predict the interfacial potential energies between a particle and collector, failure of the IFBL model to accurately calculate sticking efficiency, and failure of any model to predict the chemical and physical heterogeneity of natural systems.

2.3. Other Methods That Calculate Sticking Efficiency

There have been attempts to develop more quantitative methods to assess cell stickiness (Martin et al., 1990). Two of the most common methods are described in this section.

2.3.1. Colloid filtration method

In an empirical approach, colloid filtration theory has been used extensively to describe particle attachment to a collector surface (for example, Yao et al., 1971; Harvey and Garabedian, 1991; Gross et al., 1995; Shellenberger and Logan, 2002). Using this method, sticking efficiencies are calculated from an estimated collision efficiency and column or field influent and effluent data using the equation developed by Yao et al. (1971):

$$\alpha = \frac{4r}{3L\eta}(\theta-1)^{-1}\ln\left(\frac{N}{N_0}\right) \quad (6)$$

where N is the measured (effluent) particle concentration, N_0 is the influent particle concentration, θ is porosity, L is column length or distance, and r is radius of the collector. The difference between the influent and effluent concentrations is the number of particles that have adhered to collector surfaces. Various versions of this model have been published, each weighting differently the effects of such parameters as porosity, fluid velocity, and diffusion (Logan et al., 1995).

Using colloid filtration theory, calculated collision efficiencies and influent/effluent data are used to determine the sticking efficiency of a given system. Therefore, the sticking efficiency value obtained by colloid filtration theory is not applicable to any other system or even the same system at different physicochemical conditions. Sticking efficiency values calculated with the filtration theory often differ from measured field values by several orders of magnitude (Gregory and Wishart, 1980). The discrepancies may be due to erroneous estimates of η or errors in measuring influent and effluent particle concentrations. Also, the filtration method cannot distinguish particle removal by sorption to sediment particles from sorption to column sides nor does it include any term to describe fluid chemistry or the surface chemistries of the particle and collector.

2.3.2. The kinetic energy method

Sticking efficiency has also been estimated as a function of particle kinetic energy (E_{kin}) (Ryan and Gschwend, 1994; Dong et al., 2002a, 2002b; Hahn and O'Melia, 2004):

$$\alpha = 1 - \int_{-\Delta G_{min2}}^{\infty} f(E_{kin})\,\partial E_{kin} \quad (7)$$

$$f(E_{kin}) = \frac{2}{\sqrt{\pi}kT}\sqrt{\frac{E_{kin}}{kT}}\exp\left(-\frac{E_{kin}}{kT}\right) \quad (8)$$

In the kinetic energy method, DLVO theory is used to predict the potential energy–distance landscape between a particle and a collector. The method assumes that particles become reversibly attached to a collector when trapped in a secondary energy minimum (ΔG_{min2}). The sticking efficiency is inversely related to the probability that a particle's kinetic energy is great enough to escape from ΔG_{min2}. This method assumes that particle kinetic energy can be described by the Maxwell distribution function and that DLVO theory accurately predicts the potential energy landscape between the particle and collector (Dong et al., 2002b). Tangible estimates of α have been predicted using the kinetic energy method and a latex microsphere-glass collector system ($\alpha = 0.02$, Dong et al., 2002b; $\alpha \approx 0.01$, Hahn and O'Melia, 2004).

The kinetic energy method of determining α is markedly different from the IFBL model and colloid filtration method in that it describes particle adhesion as a reversible process. Certainly both irreversible and reversible adhesion occur in most natural systems; however, the standard model implies that reversible adhesion is a transition step toward irreversible adhesion (Marshall et al., 1971). The apparent success of the kinetic energy method suggests that in some conditions reversible adhesion, rather than irreversible adhesion, more accurately models column-scale experimental results of particle transport. For field-scale studies, however, irreversible adhe-

sion should more accurately describe particle transport (Marshall et al., 1971).

3. METHODS

3.1. Materials

Enterococcus faecalis (previously *Streptococcus faecalis*) was chosen for investigation because of its rigid spherical form which makes it well suited for attachment to AFM cantilevers. Previous studies have shown that some rod-shaped bacteria have distinctly different adhesive properties that are dependent on their orientation (Jones et al., 2003) therefore we investigate only cocci-shaped bacteria in this study. *E. faecalis* is a gram-positive, non-spore forming, nonflagellated coccus measuring ~1 μm in diameter. Gram-positive cells are rigid and robust, which makes them ideal for imaging using scanning electron microscopy (SEM), whereas gram-negative cells are less likely to survive the imaging process. *E. faecalis* is a common soil and groundwater microorganism and has been used as an indicator organism to predict sources of fecal contamination. It is a facultative anaerobe that inhabits the intestinal track of humans and other warm-blooded animals. *E. faecalis* is not known to cause disease in healthy adult humans and is classified a biosafety level 1 organism by the American Type Culture Collection.

Fisher-brand glass coverslips were used as collector material in all experiments. Silica glass was selected because it has many similarities to quartz which is an abundant mineral in unconsolidated terrestrial sediment. Both silica glass and quartz have fairly low solubility in waters of near-neutral pH and similar points of zero charge (Langmuir, 1997). Although the IFBL model is derived specifically for spherical collectors, flat collectors are used in this study. Preliminary experiments using spherical collector surfaces were not reproducible owing to piezo drift; it was not possible to consistently measure forces normal to the curved surface. In this study, flat collectors represent spherical particles that have a radius of curvature that is much larger than the *E. faecalis*. According to the Derjaguin approximation (Derjaguin, 1934), this estimate yields less than 10% error in calculated interaction forces when the collector radius is more than 10 times greater than the particle radius.

3.2. Material Preparation

Glass coverslips that were used as collectors were cleaned before all experiments in a 3:1 H_2SO_4/H_2O_2 piranha solution for 30 min to remove any possible organic contamination on the surface. Cleaned glass collectors were rinsed in copious amounts of milli-Q water following cleaning and then stored in 95% ethanol. Collectors were rinsed again with milli-Q water and dried before AFM experiments.

E. faecalis cells were grown aerobically without shaking in tryptic soy broth at 37°C. Cells were harvested at midgrowth phase and rinsed in triplicate by centrifugation using sterile milli-Q water. Cells were resuspended in sterile milli-Q water for temporary storage. Cells were stained before their isolation onto cantilevers using the Live/Dead BacLight viability kit (Molecular Probes). The viability stain colors live/viable cells green and nonviable cells red.

To improve bacterial adhesion, tipless silicon nitride AFM cantilevers (Veeco) were functionalized using 3-aminopropyltriethoxysilane (APTES). The APTES treatment generates a surface coating of amino groups on the cantilever that bind to aldehyde and ketone groups that are present on the bacterial wall (Karrasch et al., 1993). Cantilevers were soaked in 5% APTES for 30 min and then rinsed in acetone. Cells were attached to the ends of the APTES-treated cantilevers by lowering the cantilever onto a dilute solution of *E. faecalis* cells until just one or two viable cells were attached to the apex of the cantilever. Field emission scanning electron microscopy (FESEM; Leo 1550) was used to image the cantilevers and determine the exact number and position of cells on the cantilever (Fig. 2). By using a low-voltage electron beam, it was possible to image the sample without any coating before and after AFM experiments.

In these experiments, three treated cantilevers with one or two attached cells were used to collect force measurements in aqueous solutions of varying pH and ionic strength to test the effects of solution chemistry on sticking efficiency. Buffered aqueous solutions were prepared using sodium acetate and acetic acid to final pH values of 4, 5, 6, and 7. The ionic strengths of each buffered solution were adjusted to 0.05, 0.01, or 0.005 M.

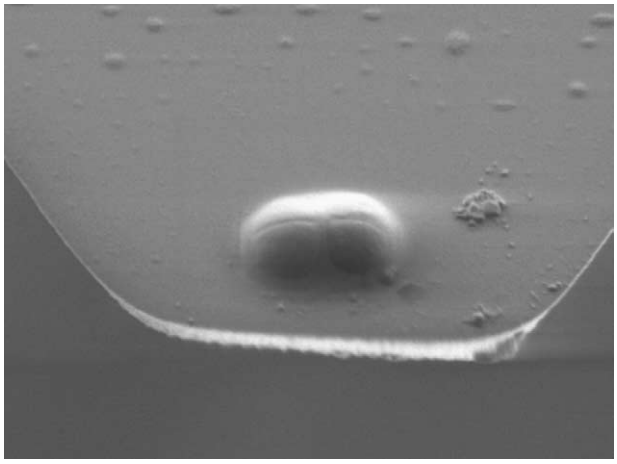

Fig. 2. FESEM image of two *E. faecalis* cells attached to an APES-treated silicon nitride cantilever. Each cell is ~1 μm in diameter.

3.3. Zeta-Potential Measurements

The ζ-potentials of *E. faecalis* and glass were measured in each buffered solution using a Malvern Instruments Zetasizer 3000HS. The piranha-cleaned glass coverslips were ground to a fine powder using an agate mortar and pestle and suspended in the buffered solutions. Cells were grown to midlog phase and rinsed three times in sterile milli-Q water before being resuspended in the buffered solutions for ~30 min to one hour before ζ-potentials were measured. The zeta-potentials were measured in duplicate sets of 5 measurements. The data sets were pooled and the average results showing standard deviation are presented.

3.4. Atomic Force Microscopy Experiments

AFM experiments were conducted using a Nanoscope IIIa Digital Instruments Multimode SPM in contact mode at room temperature. The spring constants of the cantilevers were measured using the Cleveland method before data collection but after cell attachment (Cleveland et al., 1993) and were found to be equal to the manufacturer's value (0.06 N/m). Three tipless cantilevers with attached cells were used to collect several hundred force curves for this study.

AFM data were collected as the collector glass approached, made contact with, and then separated from the cantilever at a rate of 600 nm/s, beginning at a maximum separation distance of 300 nm. The approach velocity is consistent with other AFM studies (e.g., Lower et al., 2000), comparable to motile bacterial velocities (Marshall, 1976), and a reasonable estimate of colloidal velocities through fine porous media (Nagasaki et al., 1993). AFM data were collected in each buffered solution under identical conditions. Tens to hundreds of force curves were collected in each solution to ensure reproducibility and the averaged results are presented.

Control experiments were conducted using naked cantilevers and cantilevers treated with APTES. Naked cantilevers experience strong repulsive forces (up to 0.5 nN) at separation distances between 6 and 10 nm in solutions with pH ≥5. Cantilevers that had been treated with APTES experienced no measurable repulsive forces and strong attractive forces toward the glass surface at separation distances smaller than 500 nm.

3.5. Data Processing

Up to 100 force curves were collected for the *E. faecalis*–glass system in each buffered solution. Each force curve was analyzed

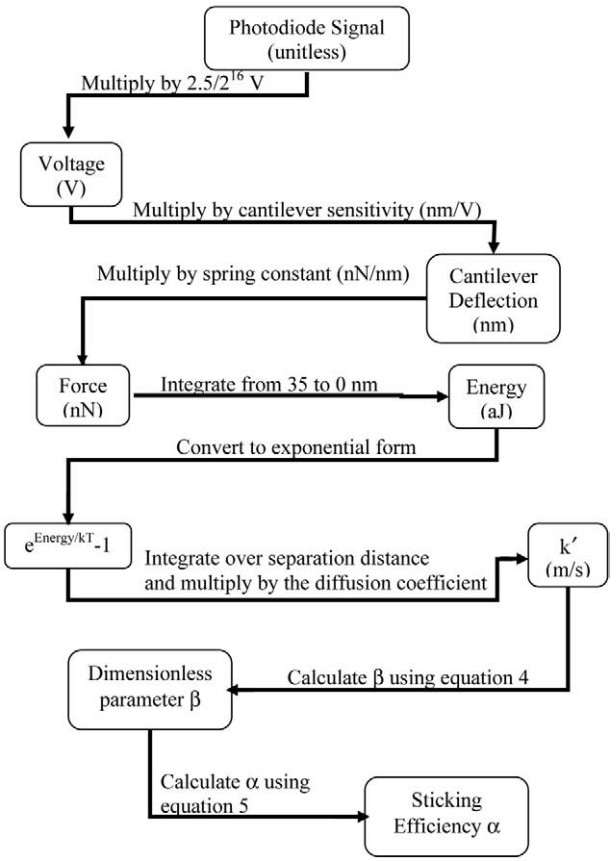

Fig. 3. Flow chart showing AFM data processing and the steps involved in calculating sticking efficiency.

individually and those that displayed significant noise owing to the presence of air bubbles (expressed as large plateaus), excess laser light (expressed as periodic oscillations), or a positive or negative slope in the region of no contact were discarded. Generally noise was minimal but increased at larger distances from separation. Scatter in the AFM data are small and results are reproducible to within ±0.1 nN in force and ±5 nm in distance. The average force curves from each data set were used to calculate sticking efficiencies for each buffered solution.

AFM data were collected as photodiode counts vs. piezo displacement in the z direction and processed into force vs. distance of separation curves using an IGOR Pro routine (WaveMetrics) and the method outlined by Kendall and Hochella (2003). The steps involved in converting raw AFM data into force curves and ultimately into sticking efficiencies are outlined in Figure 3. Interfacial potential energies vs. distance of separation profiles were calculated from force-distance curves by integration:

$$\text{Energy } (\phi) = \int_{35}^{0} \text{Fdx} \qquad (9)$$

The force curves were integrated using the trapezoid rule from a separation distance of 35 nm to the point of contact (Fig. 4). The 35 nm boundary condition was chosen based on the lack of any significant particle-collector interaction at separation distances greater than 35 nm. Only one data set displayed any interaction beyond 35 nm of separation and, for unrelated reasons to be discussed later, those data were not used to calculate sticking efficiencies. To determine the influence of the jump-to-contact region of the approach curve (Fig. 4) on calculated potential energies, force curves were also integrated from 35 nm of separation to the jump-to-contact distance. Results are identical using both regions of integration.

Exponential energy curves (Fig. 5) were derived from the interfacial potential energy curves and integrated to determine the surface reaction rate coefficient k' for each experimental condition. The sticking efficiency value that corresponds to each average force curve was calculated using Eqns. 2–5. Sticking efficiencies were calculated using the reaction rate, k', from the original IFBL model (Eqn. 2), as well as using the correction suggested by Dahneke, 1974 (Eqn. 3).

3.6. DLVO calculations

Classical DLVO theory was used to calculate energy profiles of the *E. faecalis*–glass system in identical chemical conditions. Calculations were made using ζ-potentials measured in this study and a Hamaker constant of 4.1×10^{-21} J (Dong et al., 2002b). Calculations were completed using the Derjaguin approximation (Derjaguin, 1934) and the electrostatic double layer interaction (Elimelech et al., 1998; Evans and Wennerstrom, 1999). Sticking efficiencies were calculated using the DLVO energy curves following exactly the same method that was outlined in the previous section.

4. RESULTS AND DISCUSSION

4.1. ζ-Potential

The measured ζ-potentials of *E. faecalis* and glass are presented in Figure 6. Both the bacterial cells and the glass surfaces have negative surface potentials in all solutions tested. The ζ-potentials of the glass collector are consistent with DLVO theory and become more positive with decreasing pH and with increasing ionic strength. The ζ-potentials of the *E. faecalis* cells do not change appreciably as pH is varied from 4 to 7 but do react to changes in solution ionic strength (Fig. 6B). As solution ionic strength decreases, bacterial ζ-potentials become more negative. The insensitivity of bacterial ζ-potential to changes in solution pH is possibly a reflection of the numerous types of functional groups with low dissociation constants that are present on the bacterial surface (Rijnaarts et al., 1999).

4.2. AFM Experiments

The average force curves of the *E. faecalis*–glass collector system in seven different aqueous solutions over a pH range from 4 to 7 and three different solution ionic strengths are presented in Figure 7. The force profiles collected as the particle and collector approach each other are of particular interest to this study because they contain information about the potential energy between the surfaces and can be used to predict sticking efficiency using the IFBL model.

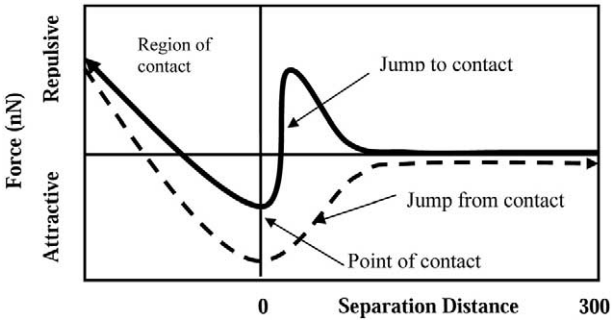

Fig. 4. Schematic force vs. distance curves as measured using AFM on approach (solid) and retraction (dashed) from a surface. Repulsive forces are assigned positive values and attractive forces are assigned negative values.

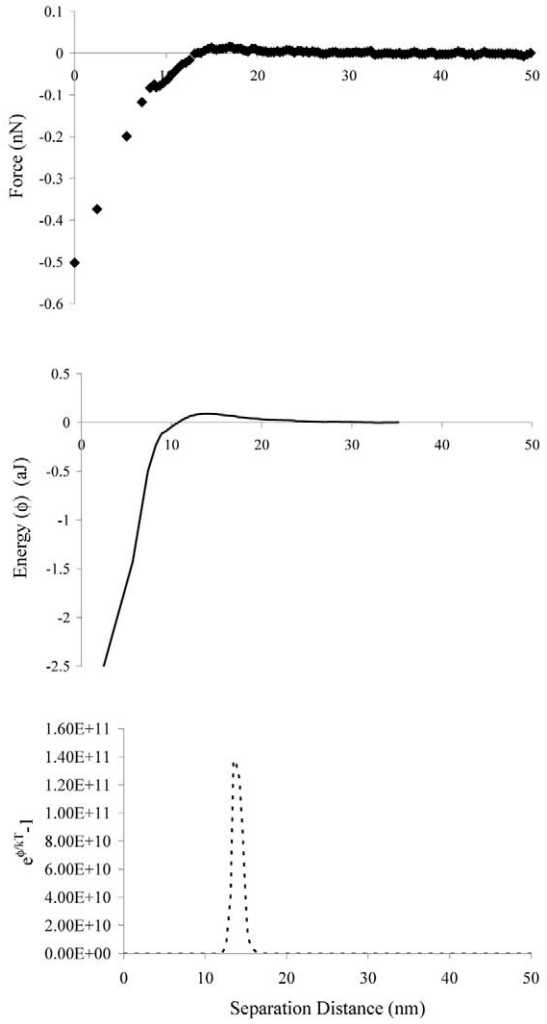

Fig. 5. Plots showing force (nN) measured by AFM, energy (aJ) calculated from the force curve, and exponential energy (unitless) calculated from the energy profile vs. *E. faecalis*-glass collector separation distance (nm). These results are for data collected at pH 5 and IS = 0.005 M. The exponential energy curve is used to calculate the surface reaction rate (Eqns. 2 and 3) which is, in turn, used to calculate sticking efficiency.

Few measurable forces of interaction were detected by AFM on approach until separation distances were smaller than 35 nm. Only in solutions of pH 4 is there any observed interaction between the *E. faecalis* and glass surfaces at separation distances greater than 35 nm. In these acidic conditions and at high ionic strength, relatively strong adhesion forces exist between the cell and glass (Fig. 7D). In all other solutions of pH $\geq$5, the bacteria and glass exert a weak repulsive force that occurs at a separation distance between 35 and 20 nm. The repulsive forces are very weak and measure less than 0.5 nN in all experiments. At shorter distances of separation the nanoscale interaction between the bacteria and glass changes from repulsive to attractive and at separation distances smaller than 20 nm the gradient of the attractive force becomes larger than the cantilever spring constant and the bacteria and glass surfaces jump into contact. This jump-to-contact region (Fig. 4) has a slope that is equal to the cantilever spring constant (Fig. 7A).

The magnitude of the maximum attractive force measured on approach is a function of solution chemistry; the force increases with decreasing pH and increasing ionic strength and correlates to measured ζ-potentials. It is therefore likely that electrostatic forces dominate the interaction occurring between the surfaces. Electrostatic forces are long-range interactions which are very sensitive to changes in both solution pH and ionic strength (Israelachvili, 1992) and arise when the distribution of counter ions surrounding two surfaces overlap. The magnitude of the force is altered by changing solution pH, because the distribution of counter ions is sensitive to pH. Also, the counter ion double layer shrinks at higher solution ionic strength, thereby reducing the separation distance at which particles and surfaces interact. Other forces that may contribute to the attractions and repulsions measured between the bacteria and glass include van der Waal's, hydrophobic, hydration, and hydrodynamic interactions (Cappella and Dietler, 1999).

The force profiles measured as the surfaces are separated also have notable features. All the retraction curves collected in this study exhibit a strong adhesive force and a major jump-off-contact event with a constant slope (Fig. 4). The jump-off-contact occurs when the cantilever spring constant is larger than the gradient of the attractive force between the cell and the glass surface. As the cantilever breaks away from the surface to reach equilibrium, the recorded cantilever deflections are a function of the spring constant (Fig. 7A). The magnitude of the adhesive force experienced upon retraction is always greater than the magnitude of the attractive force experienced upon approach (Cappella and Dietler, 1999). These differences may be attributed to the amount of surface area involved in the interaction or may be the result of polymer bridging. Cappella and Dietler (1999) provide a complete review and interpretation of force curves.

Our data indicate that the magnitude of the adhesive forces measured as the surfaces separate is a function of solution chemistry. In general, adhesion is negatively correlated to solution pH and positively correlated to solution ionic strength. At pH 4 and ionic strength equal to 0.01 M, the magnitude of the adhesive force is so large that it is impossible to pull the bacterium off the glass surface using a ramp distance of 300 nm. The adhesion is likely caused by varying surface potential on both the particle and collector surfaces. As pH decreases, the ζ-potential of the glass surface becomes significantly less negatively charged and less repulsive to the negatively charged bacterial cell. Also, at higher ionic strength the Debye length shrinks, decreasing the separation distance at which particles interact. Similar results have been shown in another study that measures the force of attraction between bacterial cells and mineral surfaces (Lower et al., 2000).

Secondary energy minima were not identified in any force profiles measured in this study. It is possible that secondary energy minima might be detected using a more sensitive cantilever; however, the large adhesive forces in this system may overpower the signal from the secondary energy minimum. The force data measured in this study indicate that adhesive forces are strong and adhesion should be dominated by irreversible deposition in the primary energy minimum.

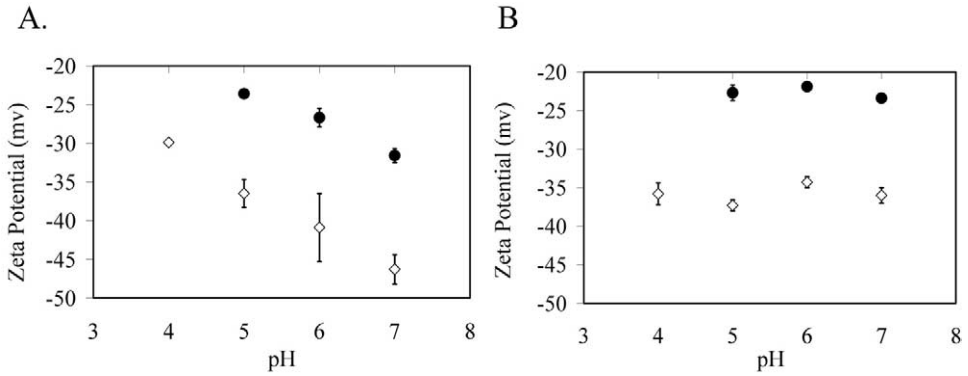

Fig. 6. The measured ζ-potentials of (A) glass and (B) *E. faecalis* in several aqueous solutions. The results shown are average values with standard deviation. Circles, IS = 0.05; diamonds, IS = 0.005. The ζ-potentials measured at an intermediate ionic strength (IS = 0.01) fell between the high and low ionic strength values.

4.3. DLVO Profiles

Force profiles were derived from the energy curves calculated using classic DLVO theory for a visual comparison with the AFM data. The calculated force curves are presented in Figure 8. Although the calculated forces show the same trends of increasing repulsive forces and decreasing attractive forces with more basic pH and lower ionic strength, there are significant differences in the two profiles. In each solution the maximum repulsive force calculated by DLVO is significantly greater (>0.5 nN) than the force measured directly using AFM. DLVO theory predicts smaller attractive forces and interactions between the bacteria and glass surface at much smaller distances of separation than are measured using AFM. Secondary energy minima are notably absent in the DLVO-generated force profiles.

The differences between calculated and measured forces in this study may be due to surface roughness and/or heterogeneity of bacterial and collector surfaces (Elimelech and O'Melia, 1990b). DLVO calculations assume perfectly smooth and homogeneous particle and collector surfaces which are unrealistic

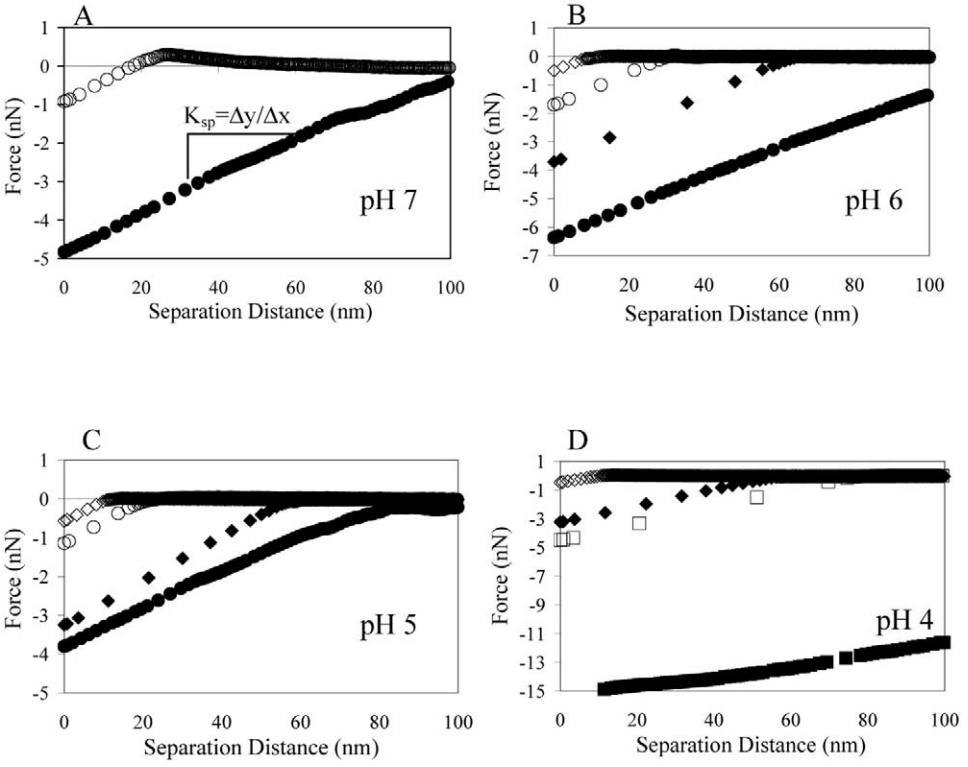

Fig. 7. Average force-distance curves for *E. faecalis* and silica glass in aqueous solutions of varying ionic strength and pH. Circles, IS = 0.05 M; squares, IS = 0.01 M; diamonds, IS = 0.005 M. Open symbols designate approach curves and closed symbols represent retraction curves. + = repulsive; − = attractive.

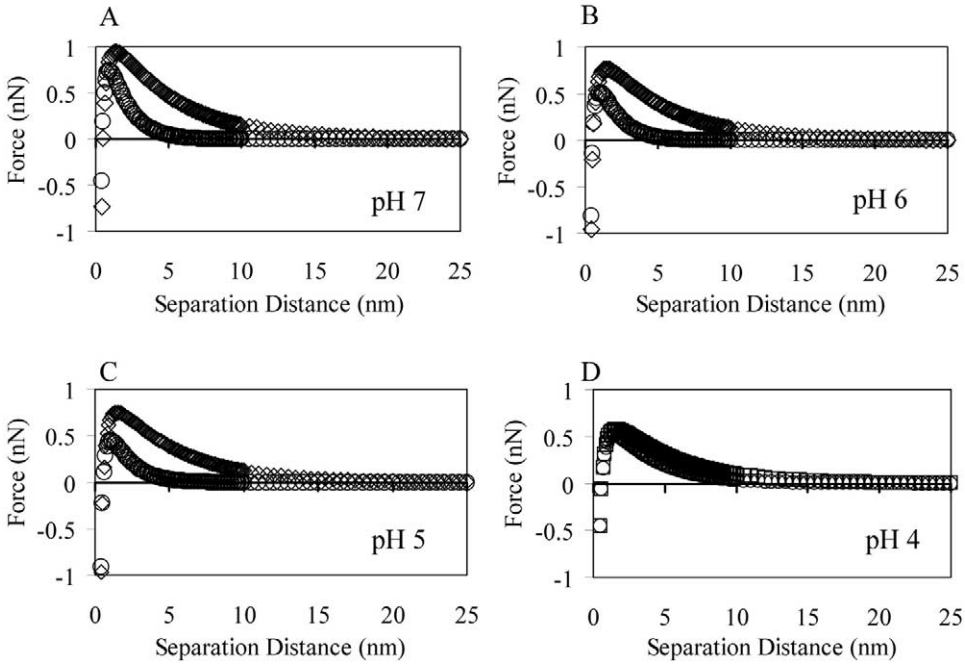

Fig. 8. Calculated force vs. distance profiles using classic DLVO theory for *E. faecalis* and silica glass in aqueous solutions of varying ionic strength and pH. Note that the scale of these plots is smaller than those in Figure 7. Circles, IS = 0.05 M; squares, IS = 0.01 M; diamonds, IS = 0.005 M.

in most natural systems. The force curves measured directly using AFM, however, do not make assumptions about either surface. It has also been postulated that charged particles in suspension may be affected by hydrodynamic drag, thereby affecting the lateral extent of charge and possibly altering double layer interactions in comparison to solutions with very little fluid movement (Elimelech and O'Melia, 1990b).

4.4. Sticking Efficiencies

The sticking efficiencies calculated using the averaged force curves of each buffered solution are presented in Table 1. Sticking efficiencies were calculated using both the original equations of the IFBL model and the modified equations by Dahneke (1974). Because no repulsive forces were measured by AFM in the experiments conducted in solutions of pH 4, sticking efficiencies for these conditions were not calculated. According to the IFBL model the sticking efficiencies in both solutions at pH 4 are equal to 1.

The α values calculated from DLVO-generated energy curves are many orders of magnitude smaller than those calculated from AFM measurements; sticking efficiencies are essentially 0 in each chemical condition investigated. Indeed, α values are drastically lower than most published experimental sticking efficiencies (Elimelech and O'Melia, 1990a, 1990b; Ryan et al., 1999; Dong, 2002) but are very similar to results from other purely theoretical studies (Elimelech et al., 2000; Dong et al., 2002b). The implications of these sticking efficiency values will be discussed in the following section.

Sticking efficiencies calculated using the traditional IFBL model are consistently one to three orders of magnitude larger than those calculated using Dahneke's correction. The correc-

Table 1. Calculated sticking efficiencies (α) in buffered solutions of varying pH and ionic strength (IS) using data measured by AFM (α_{AFM}) and data calculated using DLVO theory (α_{DLVO}). The sticking efficiencies were calculated using the original IFBL equations (IFBL α) and the hydrodynamic correction by Dahneke (Dahneke α).

	α^{AFM}		α_{DLVO}	
Solution	IFBL α	Dahneke α	IFBL α	Dahneke α
pH 7 IS 0.05	2.6×10^{-33}	3.5×10^{-35}	1.7×10^{-158}	1.69×10^{-161}
pH 6 IS 0.05	4.4×10^{-5}	2.4×10^{-6}	1.0×10^{-110}	1.09×10^{-113}
pH 5 IS 0.05	1	1	4.2×10^{-98}	4.7×10^{-101}
pH 4 IS 0.01	1	1	2.2×10^{-231}	2.66×10^{-234}
pH 6 IS 0.005	9.6×10^{-16}	2.6×10^{-17}	$<1 \times 10^{-307}$	$<1 \times 10^{-307}$
pH 5 IS 0.005	3.6×10^{-8}	9.7×10^{-10}	$<1 \times 10^{-307}$	$<1 \times 10^{-307}$
pH 4 IS 0.005	1	1	$<1 \times 10^{-307}$	$<1 \times 10^{-307}$

tion, which accounts for hydrodynamic interactions that can significantly inhibit deposition, is expected to drop the calculated sticking efficiency value as shown.

The sticking efficiencies calculated using both DLVO-derived and AFM data at high ionic strength display a distinct trend that is reflective of ζ-potential. Sticking efficiencies calculated from both data sets increase as pH decreases and as ionic strength increases. The trend is likely present at low ionic strength but is out of the calculated range of this study. In solutions of nearly neutral pH, the surface potential of glass is very strongly negative and α is low. As pH decreases and the ζ-potential of glass becomes more negative, α increases. Likewise, at constant pH and higher ionic strength, ζ-potentials become more neutral and sticking efficiencies also increase. The results are consistent with an earlier study that measured the sticking efficiencies of carboxylated polystyrene microparticles using the same method (Cail and Hochella, 2005).

4.5. Efficacy of the IFBL Model

As previously mentioned, the IFBL model has been criticized as a poor predictor of particle adhesion (Elimelech and O'Melia, 1990b; Ryan and Elimelech, 1996; Dong et al., 2002b). The sticking efficiencies calculated using this model and DLVO-generated energy curves greatly underestimate α calculated in column and field studies in nonidentical but similar systems (Elimelech and O'Melia, 1990a, 1990b; Ryan et al., 1999; Elimelech et al., 2000; Dong et al., 2002b).

To make the concept of sticking efficiency more tangible, distances of particle transport have been calculated using α determined in this study and a hypothetical soil and the rearranged filtration equation (Yao et al., 1971):

$$L = \frac{4}{3}\frac{r}{\eta(\theta-1)\alpha}\ln\left(\frac{C}{C_0}\right) \qquad (10)$$

where L is the distance traveled, r is collector grain radius (500 μm, representative of a course sand), θ is porosity (0.4), C_0 and C are initial and final particle concentrations, and α and η are sticking and collision efficiencies. For these calculations, $\eta = 0.026$ (Johnson et al., 1996). Transport distances were calculated for a range of final particle concentrations from 99% to 0.1% of C_0. The results are presented in Table 2. Field data indicate that bacterial cells and inorganic colloids behave similarly in field studies (Harvey and Bouwer, 1990); therefore they will be treated equally in this discussion.

The distances of travel associated with very small sticking efficiencies (i.e., $\alpha < 9.6 \times 10^{-16}$) are immeasurably large. For example, using a sticking efficiency of 9.6×10^{-16} and the filtration equation above, ~50% of a population of microparticles would travel a distance of 6.2×10^{8} km (~4 times the distance to the sun!). However, α derived from AFM data at high ionic strength and at pH ≤6 correspond to travel distances that range from a few mm to hundreds of meters. These distances represent the maximum attainable travel distances of colloidal particles that do not favor adhesion to the collector surface. Naturally, colloids that favor adhesion would travel much shorter distances. For example, bacterial transport distances in natural systems are expected to be much shorter, owing to heterogeneous collector surfaces that may be more favorable to adhesion, e.g., iron oxyhydroxide coatings and organic matter.

Table 2. Estimated distances of transport (note that the units of length are not consistent) corresponding to sticking efficiencies calculated using the IFBL model.

α	C/C_0	L
1×10^{-307}	.99	∞
	.50	∞
	.001	∞
9.6×10^{-16}	.99	9.0×10^{6} km
	.50	6.2×10^{8} km
	.001	6.2×10^{9} km
3.6×10^{-8}	.99	0.24 km
	.50	17 km
	.001	160 km
4.4×10^{-5}	.99	0.20 m
	.50	13 m
	.001	130 m
1	.99	0.00086 mm
	.50	0.059 mm
	.001	0.59 mm

An important observation can be made from the calculated distances displayed in Table 2 and Eqn. 10. Because of the relatively high limits of detection associated with bacterial populations (AOAC International, 1999), it is increasingly difficult to accurately measure sticking efficiencies smaller than 1×10^{-4} using columns shorter than 1 m. Laboratory scale investigations of bacterial sticking efficiency are limited by cell enumeration techniques.

The apparent success of the kinetic energy method in predicting sticking efficiencies of latex microspheres (Hahn and O'Melia, 2004) suggests that reversible adhesion may be an important process in particle removal from solution under certain conditions. For example, at near-neutral pH conditions the sticking efficiencies calculated in this study predict essentially no adhesion of the bacteria to the glass surface. Field and column data from similar systems report that significant particle removal does occur under unfavorable conditions and indicate that sticking efficiencies of these systems are much higher. If reversible adhesion were to dominate under these conditions, the IFBL model would significantly underpredict sticking efficiency by assuming all deposition is irreversible. Similarly, at low solution pH, where the IFBL model predicts high sticking efficiencies, irreversible adhesion likely dominates. Accurate predictions of sticking efficiencies and distances of colloidal particle transport in natural systems might be improved by accounting for both short-term reversible adhesion and long-term irreversible adhesion.

The sticking efficiency values calculated using the IFBL model in this study are sensitive to small changes in interfacial potential energy. The potential energy profiles calculated using DLVO theory have larger maximum energy values which correlate to much smaller sticking efficiencies compared to AFM results. This observation may limit the application of the IFBL model to systems that are adequately described by theory or are conducive to AFM measurements. Small errors in force or energy profiles may yield significant errors in sticking efficiency.

Atomic force microscopy is a valuable tool for predicting the trends of increasing and decreasing α with changes in solution pH

and ionic strength, as well as for predicting distances of transport through porous media. In this study, the effects of solution chemistry on sticking efficiency were consistent and directly experimentally measurable: Lowering solution pH resulted in smaller interfacial repulsive forces and larger sticking efficiency values at both high and low solution ionic strength. Advances in AFM, including tapping mode force curve measurements (Todd et al., 2001), may improve the measurement of interfacial potential energies and provide more accurate estimates of sticking efficiency for a wider range of colloidal systems.

5. SUMMARY AND SIGNIFICANCE

The accurate prediction of particle transport in the subsurface is important to several fields in the geosciences. Empirical methods to predict particle transport in porous media are largely unsuccessful and are constrained to restricted physicochemical systems, whereas theoretical descriptions are rarely applicable to real heterogeneous systems. Laboratory-scale investigations of bacterial sticking efficiencies are limited by the accuracy of cell detection methods. This study presents a new method of calculating sticking efficiency using measurable force data. Using this AFM technique, bacterial sticking efficiencies are, for the first time, determined directly from measurable forces of interaction between the cell and collector surfaces using the IFBL model. Under certain conditions where irreversible adhesion is the predominate particle removal process and/or when combined with a term that also predicts reversible adhesion, the IFBL model may more accurately describe the transport of microparticles in porous media by incorporating the nanoscale interactions that control particle attachment and have historically been left out of consideration. Of course, the larger picture should always be considered; improved predictions of particle adhesion at the nanoscale may yield better estimates of particle transport at the field scale.

6. LIST OF SYMBOLS

α	Sticking efficiency (unitless)
η	Collision efficiency (unitless)
A_s	Happel's cell model constant (unitless)
D	Particle diffusion coefficient (m^2/s)
U	Undisturbed fluid velocity (m/s)
r	Particle radius (m)
C	Collector efficiency (unitless)
k'	Surface reaction rate coefficient (m/s)
ϕ	Intersurface potential energy (J)
k	Boltzmann's constant (J/K)
T	Temperature (K)
y	Particle-collector separation distance (m)
β	Sticking parameter defined by Eqn. 4 (unitless)
Γ	Mathematical gamma function
$S(\beta)$	Function that describes the collection of brownian particles onto a spherical collector (unitless)
L	Column length or distance (m)
θ	Porosity
N_0	Influent concentration
N	Effluent concentration
ΔG_{min2}	Secondary energy minima
E_{kin}	Particle kinetic energy
F	Force (nN)

Acknowledgments—-We thank S. Lower, D. Rimstidt, M. Schreiber, C. Tadanier and three anonymous reviewers for helpful comments and suggestions on this manuscript. S. McCarthy captured FESEM images and A. Ritter and P. Haskell assisted in mathematical analyses. This work was supported by NSF EAR-01-03053.

Associate editor: Jeremy B. Fein

REFERENCES

AOAC International. (1999) AOAC International qualitative and quantitative microbiology guidelines for methods validation. *J. AOAC Int.* **82,** 402–415.

Cail T. L. and Hochella M. F. (2005) Experimentally derived sticking efficiencies of microparticles using Atomic Force Microscopy. *Environ. Sci. Tech.* **39,** 1011–1017.

Cappella B. and Dietler G (1999) Force-distance curves by atomic force microscopy. *Surface Sci. Rep.* **34,** 1–104.

Cleveland J. P., Manne S., Bocek D., and Hansma P. K. (1993) A nondestructive method for determining the spring constant of cantilevers for scanning force microscopy. *Rev. Sci. Instr.* **64,** 403–405.

Dahneke B. (1974) Diffusional Deposition of Particles. *J. Colloid Interface Sci.* **48,** 520–522.

Derjaguin B. V. (1934) Untersuchungen uber die Reibung und Adhasio, IV. *Kolloid Z.* **69,** 155–164.

Dong H. (2002) Significance of electrophoretic mobility distribution to bacterial transport in granular porous media. *J. Microbiol. Meth.* **51,** 83–93.

Dong H. L., Onstott T. C., Deflaun M. F., Fuller M. E., Scheibe T. D., Streger S. H., Rothmel R. K., and Mailloux B. J. (2002a) Relative dominance of physical versus chemical effects on the transport of adhesion-deficient bacteria in intact cores from South Oyster, Virginia. *Environ. Sci. Tech.* **36,** 891–900.

Dong H. L., Onstott T. C., Ko C. H., Hollingsworth A. D., Brown D. G., and Mailloux B. J (2002b) Theoretical prediction of collision efficiency between adhesion-deficient bacteria and sediment grain surface. *Colloids Surf. B Biointerfaces* **24,** 229–245.

Elimelech M. and O'Melia C. R. (1990a) Effect of particle-size on collision efficiency in the deposition of brownian particles with electrostatic energy barriers. *Langmuir* **6,** 1153–1163.

Elimelech M. and O'Melia C. R. (1990b) Kinetics of deposition of colloidal particles in porous media. *Environ. Sci. Tech.* **24,** 1528–1536.

Elimelech M., Gregory J., Jia X., and Williams R. A (1998) *Particle Deposition and Aggregation: Measurement, Modeling and Simulation.* Butterworth-Heinnemann.

Elimelech M., Nagai M., Ko C. H., and Ryan J. N. (2000) Relative insignificance of mineral grain zeta potential to colloid transport in geochemically heterogeneous porous media. *Environ. Sci. Tech.* **34,** 2143–2148.

Evans D. F. and Wennerstrom H (1999) *The Colloidal Domain: Where Physics, Chemistry, Biology and Technology Meet.* Wiley-VCH.

Gregory J. and Wishart A. J (1980) Deposition of latex-particles on alumina fibers. *Colloids and Surfaces* **1,** 313–334.

Gross M. J., Albinger O., Jewett D. G., Logan B. E., Bales R. C., and Arnold R. G. (1995) Measurement of bacterial collision efficiencies in porous media. *Water Res.* **29,** 1151–1158.

Hahn M. W. and O'Melia C. R. (2004) Deposition and reentrainment of Brownian particles in porous media under unfavorable chemical conditions: Some concepts and applications. *Environ. Sci. Tech.* **38,** 210–220.

Harvey R. W. and Bouwer E. J. (1990) Limits on quantitative descriptions of biocolloid mobility in contaminated groundwater. In *Manipulation of Groundwater Colloids for Environmental Restoration* (eds. J. F. McCarthy and F. J. Wobber), pp. 57–64. Lewis Publishers.

Harvey R. W. and Garabedian S. P. (1991) Use of colloid filtration theory in modeling movement of bacteria through a contaminated sandy aquifer. *Environ. Sci. Tech.* **25,** 178–185.

Harvey R. W. and Harms H. (2002) Transport of microorganisms in the terrestrial subsurface: in situ and laboratory methods. In *Manual of Environmental Microbiology* (ed. C. J. Huerst), pp. 753–776. ASM Press.

Israelachvili J (1992) *Intermolecular and Surface Forces.* Academic Press.

Johnson W. P., Martin M. J., Gross M. J., and Logan B. E. (1996) Facilitation of bacterial transport through porous media by changes in solution and surface properties. *Colloids Surfaces A Physicochem. Eng. Aspects* **107,** 263–271.

Jones J., Feick J., Imoudu D., Chukwumah N., Vigeant M., and Velegol D. (2003) Oriented adhesion of *Escherichia coli* to polystyrene particles. *Appl. Environ. Microbiol.* **69,** 6515–6519.

Karrasch S., Dolder M., Schabert F., Ramsden J., and Engel A. (1993) Covalent binding of biological samples to solid supports for scanning probe microscopy in buffer solution. *Biophys. J.* **65,** 2437–2446.

Kendall T. A. and Hochella M. F. (2003) Measurement and interpretation of molecular-level forces of interaction between the siderophore azotobactin and mineral surfaces. *Geochim. Cosmochim. Acta* **67,** 3537–3546.

Langmuir D (1997) *Aqueous Environmental Geochemistry.* Prentice-Hall.

Levich V. G (1962) *Physicochemical Hydrodynamics.* Prentice-Hall.

Logan B. E (1999) *Environmental Transport Processes.* John Wiley and Sons.

Logan B. E., Jewett D. G., Arnold R. G., Bouwer E. J., and O'Melia C. R. (1995) Clarification of clean-bed filtration models. *J. Environ. Eng. ASCE* **121,** 869–873.

Lower S. K., Tadanier C. J., and Hochella M. F. (2000) Measuring interfacial and adhesion forces between bacteria and mineral surfaces with biological force microscopy. *Geochim. Cosmochim. Acta* **64,** 3133–3139.

Marshall K., Stout R., and Mitchell R (1971) Mechanism of initial events in sorption of marine bacteria to surfaces. *J. Gen. Microbiol.* **68,** 337–348.

Marshall K. C (1976) *Interfaces in Microbial Ecology.* Harvard University Press.

Martin R. E., Bouwer E. J., and Hanna L (1990) Cells and surfaces in groundwater systems. In *Manipulation of Groundwater Colloids for Environmental Restoration* Lewis Publishers (eds. J. F. McCarthy and F. J. Wobber), pp. 67–71.

Nagasaki S., Tanaka S., and Suzuki A. (1993) Fast transport of colloidal particles through quartz-packed columns. *J. Nucl. Sci. Tech.* **30,** 1136–1144.

Rijnaarts H., Norde W., Lyklema J., and Zehnder A (1999) DLVO and steric contributions to bacterial deposition in media of different ionic strengths. *Colloids Surfaces B Biointerfaces* **14,** 179–195.

Ryan J. N. and Elimelech M. (1996) Colloid mobilization and transport in groundwater. *Colloids Surfaces A Physicochem. Eng. Asp.* **107,** 1–56.

Ryan J. N. and Gschwend P. M. (1994) Effects of ionic-strength and flow-rate on colloid release—relating kinetics to intersurface potential energy. *J. Colloid Interface Sci.* **165,** 536–536.

Ryan J., Elimelech M., Ard R., Harvey R., and Johnson P. (1999) Bacteriophage PRD1 and silica colloid transport and recovery in an iron oxide–coated sand aquifer. *Environ. Sci. Tech.* **33** (*1*), 63–73.

Shellenberger K. and Logan B. E. (2002) Effect of molecular scale roughness of glass beads on colloidal and bacterial deposition. *Environ. Sci. Tech.* **36** 184–189.

Spielman L. A. and Friedlander S. K. (1974) Role of electrical double-layer in particle deposition by convective diffusion. *J. Colloid Interface Sci.* **46,** 22–31.

Tobiason J. E (1989) Chemical effects on the deposition of non-brownian particles. *Colloids Surf.* **39,** 53–77.

Todd B. A., Eppell S. J. and Zypman F. R. (2001) Squeezing out hidden force information from scanning force microscopes. *Appl. Phys. Lett.* **79,** 1888–1890.

Whitman W. B., Coleman D. C., and Wiebe W. J. (1998) Prokaryotes: The unseen majority. *Proc. Natl. Acad. Sci. U. S. A.* **95,** 6578–6583.

Yao K. M., Habibian M. M. and O'Melia C. R. (1971) Water and waste water filtration—concepts and applications. *Environ. Sci. Tech.* **5,** 1105–1112.